International Journal of Current Engineering and Technology
E-ISSN 2277 – 4106, P-ISSN 2347 – 5161

Available at http://inpressco.com/category/ijcet

Research Article

Heat and Mass transfer of magnetohydrodynamic pulsatile Flow of Casson Fluid with couple stress through Porous medium

Nabil.T.M.El-dabe, Galal M.Moatimeid, Mohamed.A .Hassan and Ehab.S.Ashour*

Mathematics Department, Faculty of Education, Ain shams, Univrsity, Heliopolis, Cairo, Egypt

Accepted 10 Aug 2016, Available online 15 Aug 2016, Vol.6, No.4 (Aug 2016)

Abstract

We have analyzed the MHD flow of a conducting couple stress fluid in oscillating channel with heat and mass transfer. The non-Newtonian fluid under consideration is obeying the Casson model. In this analysis we are taking into account the induced magnetic field. The analytic solution for the problem has been obtained by using homotopy perturbation method for steady and unsteady cases. The distributions, temperature of the velocity and concentration functions are discussed. The effects of the various parameters such as the couple stress parameter, the Hartmann number M^2, the Reynolds number R_e and heat and mass transfer coefficient. It was found that the Darcy's coefficient for the fluid restrain the velocity. Vise versa Hartmann number M^2, the Reynolds number R_e haste of it.

Keywords: *MHD flow, Casson Fluid etc.*

1. Introduction

The study of a couple stress fluid is very useful in understanding various physical problems, because it possesses the mechanism to describe rheologically complex fluids such as liquid crystals, colloidal fluids, liquids containing long-chain molecules as polymeric suspensions, animal and human blood and lubrication Kh. Mekheimer. A. Khalid *et al.* studied the unsteady MHD free flow of a Casson fluid past an oscillating vertical plate wsith constant wall temperature. a magnetohydrodynamic (MHD) three dimensional Casson fluid flow past a porous linearly stretching sheet is investigated, introducing convective boundary condition at the surface where the thermal conductivity of the fluid varies linearly with respect to the temperature. Is investigated by G. Mahanta. The unsteady two-dimensional flow of a non-Newtonian fluid over a stretching surface having a prescribed surface temperature is investigated by S. Mukhopadhyay. N. Ahmed studied the Squeezing flow of an electrically conducting Casson fluid with The laws of conservations under the similarity transformation suggested by Wang (1976) have been used to extract a highly nonlinear ordinary differential equation governing the magnetohydrodynamic (MHD) flow. S. Gupta studied Heat and mass transfer with a solid surface to a fluid undergoing pulsatile flow, consisting of sinusoidal pulsations superimposed on a mean flow. Heat and mass transfer phenomena were studied in the sudden expansion region of a pipe under steady and pulsatile conditions is studied by P. Ma. G. Shit investigated the Unsteady flow of blood and heat transfer characteristics in the neighborhood of an overlapping constricted artery have been investigated in the presence of magnetic field and whole body vibration. S. Srinivas investigates the effects of chemical reaction and Soret effects on hydromagnetic laminar viscous pulsating flow in a porous channel with slip and convective boundary conditions.

The purpose of the present investigation is to study the pulsatile flow of couple-stress non-Newtonian fluid obeying Casson model through a porous medium with heat and mass transfer in two-dimensional channel. The system is subjected to a transverse uniform magnetic field in the presence of the effect of chemical reaction. The analytical solutions for motion, heat and concentration equations are obtained by using homotopy perturbation technique. The effect of the problems parameters on those solutions are discussed and illustrated graphically. To clarify the problem, the article is organized as follows: In Section2, the physical description of the problem including the basic equations that govern the motion is presented. Section 3 is devoted to introduce the basic equations together with the linear boundary conditions. The method of solution according to the homotopy perturbation technique was presented in Section 4. Section 5, we derived the transition curves and gives a discussion of the steady pictures according to the relative velocity and many parameter. Finally, in Section 6, we give concluding remarks for this study based on the obtained results.

*Corresponding author: **Ehab.S.Ashour**

2. Mathematical formulation and solution

Consider the pulsatile transport of an incompressible Bi-viscosity fluid in a two dimensional plates of width (h) as shown in figure (1). The fluid is being injected by one plate with constant velocity V_0 and sucked off by the other plate with the same velocity. A uniform magnetic field with magnetic flux density vector $B = (0, B_0, 0)$ is applied. Also The heat and mass transfer in the channel are taken into account by giving temperature and concentration to the lower and upper plate as T_0, C_0 and T_w, C_w respectively.

Cartesian coordinates are selected so as to make the x-axis in the direction of the flow and y-axis in the direction normal to the mean position of the channel.

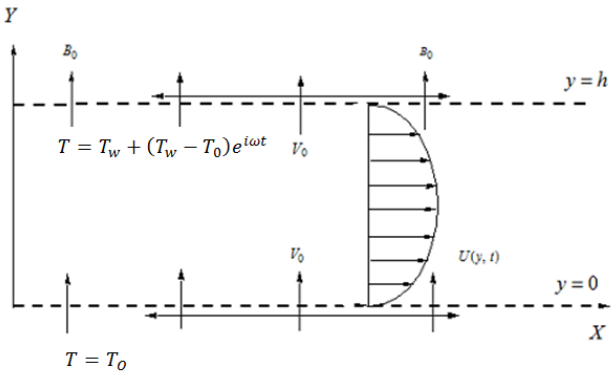

Fig 1: Geometry of the problem

The constitutive equation of the Bi-viscosity model can be written in the following tensor notation as:

$$\tau_{ij} = 2\left(\mu_B + P_y\sqrt{2\pi c}\right) \quad (1)$$

$$e_{ij} = \frac{1}{2}\left(\frac{\partial u_i}{\partial x_j} + \frac{\partial u_j}{\partial x_i}\right) \quad (2)$$

Where μ_B is the plastic viscosity, P_y is the yielding stress, $\pi = e_{ij}e_{ij}$, which e_{ij} is the i, j component of the deformation rate and the value of β denotes the upper limit of apparent viscosity coefficient. For Newtonian fluid. $P_y = 0$ Where u, V_0 are the for unsteady two-dimensional flows, the velocity, temperature and concentration can be written as a function of y *and* t.

The viscoelastic fluid in x-direction is driven by a pulsatile pressure gradient

$$\frac{\partial p^*}{\partial x} = A^* + B^* e^{i\omega t} \quad (3)$$

Where A^* and B^* are known quantities represents the steady-state of the pressure gradient and oscillatory parts respectively where ω is the frequency of pulsatile flow.

3. Basic equations

The equations governing the flow of an incompressible viscoelastic fluid are given by:

The continuity equation

$$\nabla.\underline{V} = 0 \quad (4)$$

The momentum equation

$$\rho\left[\frac{\partial V}{\partial t} + (\underline{V}.\nabla)V\right] = -\nabla P + \nabla.\underline{\tau} + \mu_e\left(\underline{J}\wedge\underline{B}\right) - \frac{\mu}{k_p}\underline{V} - \eta\nabla^4\underline{V} \quad (5)$$

The temperature equation with radiation

$$c_p\rho\left[\frac{\partial T}{\partial t} + (\underline{V}.\nabla)T\right] = k_0\nabla^2 T - \nabla.q_r - \mathrm{Q\,T} \quad (6)$$

The concentration equation with diffusion and chemical reaction

$$\left[\frac{\partial C}{\partial t} + (\underline{V}.\nabla)C\right] = D_m\nabla^2 C + \frac{D_m k_T}{T_m}\nabla^2 T - \zeta C \quad (7)$$

Where $\underline{V}$ is the velocity, ρ is the liquid density, μ is the viscosity of the fluid, k_p is the permeability of the porous medium, τ is the extra stress tensor obeying Casson model, P is the pressure. A uniform magnetic field with magnetic flux density vector $\underline{B} = (0, B_0, 0)$ is applied, μ_e permeability of magnetic field , $\underline{J}$ is current density. T and C temperature and concentration of the fluid, k_0 is the coefficient of thermal conductivity, c_p is the specific heat capacity at constant pressure and D_m is the coefficient of mass diffusivity, k_T thermal diffusivity , $q_r = \frac{4\sigma_0}{3K}\frac{\partial T}{\partial y} \simeq \frac{16\sigma_0 T_2^3}{3K}\frac{\partial T}{\partial y}$ is the radiative heat flux , where σ_0 is the Stefan-Boltzman constant , K is the mean absorption coefficient T_m is the mean temperature , Q is heat flux ,ζ is constants of chemical reaction. Thus, for the effect of couple stress to be present $V_{i,rrss}$ must be nonzero.

For unsteady two-dimensional flow, the velocity, temperature and concentration can be written as a function of y and t only.

$$V = (u(y,t), V_0). \quad (8)$$

$$T = T(y,t),\ C = C(y,t) \quad (9)$$

where u *and* V_0 be the longitudinal and transverse velocity components of the fluid, respectively.

Equations (5-8) reduce to

$$\frac{\partial u}{\partial x} = 0 \quad (10)$$

$$\frac{\partial u}{\partial t} + V_0\frac{\partial u}{\partial y} = -\frac{1}{\rho}\frac{\partial p}{\partial x} + \mu_B(1+\beta^{-1})\left(\frac{\partial^2 u}{\partial y^2}\right) - \frac{\sigma B_0^2}{\rho}u - \frac{\nu}{k_p^*}u - \eta\left(\frac{\partial^4 u}{\partial y^4}\right) \quad (11)$$

$$\frac{\partial T}{\partial t} + V_0\frac{\partial T}{\partial y} = \frac{k_0}{c_p\rho}\left(\frac{\partial^2 T}{\partial y^2}\right) + \frac{16\sigma_0 T_2^3}{3K}\frac{\partial}{\partial y}\left(\frac{\partial T}{\partial y}\right) - \mathrm{Q\,T} \quad (12)$$

$$\frac{\partial \mathrm{C}}{\partial \mathrm{t}} + V_0 \frac{\partial C}{\partial y} = D_m \left(\frac{\partial^2 \mathrm{C}}{\partial \mathrm{y}^2}\right) + \frac{D_m k_T}{T_m} \frac{\partial^2 T}{\partial y^2} - \zeta\, C \qquad (13)$$

In mathematical form, the corresponding boundary conditions can be put as

$$\left.\begin{array}{llll} u = V_0 e^{iwt}, & T = T_w + e^{iwt}(T_w - T_0) & C = C_w + e^{iwt}(C_w - C_0) & at \quad y = h \\ u = V_0 e^{iwt}, & T = T_0 & C = C_0 & at \quad y = 0 \end{array}\right\} \qquad (14)$$

Let us introduce the following dimensionless quantities as follow:

$$\left.\begin{array}{lll} y^* = \frac{y}{h} & u^* = \frac{u}{V_0}, & t^* = \frac{t\,V_0}{h} \\ R_e = \frac{V_0 h}{\nu}, & k_p = \frac{k_p^*}{\rho\ h^2}, & T^* = \frac{T - T_0}{T_w - T_0}, \\ c^* = \frac{C - C_0}{C_w - C_0}, & p^* = \frac{hp}{\rho \nu V_0}, & M^2 = \frac{\sigma\ h^2 B_0^2}{\rho \nu}, \\ S_c = \frac{\nu}{D_m} & S_r = \frac{D K_T (T_w - T_0)}{\nu\, T_m (C_w - C_0)} & p_r = \frac{V_0 c_p h\, \rho}{k_0} \\ \omega^* = \frac{\omega\, h}{V_0} & & \end{array}\right\} \qquad (15)$$

Where R_e is the Reynolds number, M^2 is the magnetic field parameter, p_r is the Prandtle number, S_c is the Schmidt number, S_r is the Soret number and E_c the Eckhart number.

The system of equations (11-13) with the condition (15) can be written in dimensionless form after dropping star mark as follows:

$$R_e \left(\frac{\partial u}{\partial t} + \frac{\partial u}{\partial y}\right) = -\frac{\partial p}{\partial x} + \frac{1}{R_e}(1 + \beta^{-1}) \left(\frac{\partial^2 u}{\partial y^2}\right) - \left(M^2 + \frac{1}{k_p}\right) u - \frac{1}{R_c} \left(\frac{\partial^4 u}{\partial y^4}\right) \qquad (16)$$

$$R_e p_r \left(\frac{\partial T}{\partial t} + \frac{\partial T}{\partial y}\right) = \left(1 + \frac{4}{3R_n}\right) \left(\frac{\partial^2 T}{\partial y^2}\right) - \gamma\, T \qquad (17)$$

$$R_e \left(\frac{\partial \mathrm{C}}{\partial \mathrm{t}} + \frac{\partial \mathrm{C}}{\partial \mathrm{y}}\right) = \frac{1}{S_c} \left(\frac{\partial^2 \mathrm{C}}{\partial \mathrm{y}^2}\right) + S_r \left(\frac{\partial^2 T}{\partial y^2}\right) - \xi C \qquad (18)$$

Where R_c is the couple stress parameter and R_n is the radiation parameter.

The corresponding dimensionless boundary conditions are:

$$\left.\begin{array}{llll} u = e^{i\omega t}, & T = 1 + e^{i\omega t} & C = 1 + e^{i\omega t} & at \quad y = 1 \\ u = e^{i\omega t}, & T = 0 & C = 0 & at \quad y = 0 \end{array}\right\} \qquad (19)$$

4. Solution of the problem

To solve equations ((16)- (18)) subjected to the boundary conditions (19), we write the velocity, temperature and concentration in the form:

$$u = u_s(y) + u_f(y) e^{i\omega t} \qquad (20)$$

$$T = T_s(y) + T_f(y) e^{i\omega t} \qquad (21)$$

$$C = C_s(y) + C_f(y) e^{i\omega t} \qquad (22)$$

Equations ((16)-(18)) take the following form:

4.1 Steady case

$$-\frac{1}{R_c} u_s^{\backslash\backslash\backslash\backslash} + \alpha_2 u_s^{\backslash\backslash} + R_e u_s^{\backslash} - \alpha_1 u_s = A \qquad (23)$$

$$\left(1 + \frac{4}{3R_n}\right) T_s^{\backslash\backslash} - R_e p_r T_s^{\backslash} - \gamma\, T_s = 0 \qquad (24)$$

$$\frac{1}{S_c} \mathrm{C}_s^{\backslash\backslash} - \mathrm{C}_s^{\backslash} - \xi\, C = -S_r T_s^{\backslash\backslash} \qquad (25)$$

4.2 Unsteady case

$$-\frac{1}{R_c} u_f^{\backslash\backslash\backslash\backslash} + \alpha_2 u_f^{\backslash\backslash} - R_e u_f^{\backslash} - (\alpha_1 + i\omega R_e) u_f = B \qquad (26)$$

$$\left(1 + \frac{4}{3R_n}\right) T_f^{\backslash\backslash} - R_e P_r T_f^{\backslash} - (\gamma + i\omega R_e P_r)\, T_f = 0 \qquad (27)$$

$$\frac{1}{S_c} \mathrm{C}_f^{\backslash\backslash} - \mathrm{C}_f^{\backslash} - \xi\, \mathrm{C}_f = -S_r T_f^{\backslash\backslash} \qquad (28)$$

Equations ((23)-(28)) can be solved by using the following perturbation method for small homotopy perturbation parameter (q),

$$u_s(y) = u_{s0}(y) + q\, u_{s1}(y) + O(q) \qquad (29)$$

$$u_f(y) = u_{f0}(y) + q\, u_{f1}(y) + O\,(q) \qquad (30)$$

Collecting the coefficients of like power of (q), we get the following set of equations of motion:

$$\alpha_2 u_{so}^{\backslash\backslash} - R_e u_{so}^{\backslash} - \alpha_1 u_{so} = A \qquad (31)$$

$$\alpha_2 u_{s1}^{\backslash\backslash} - R_e u_{s1}^{\backslash} - \alpha_1 u_{s1} = -u_{s0}^{\backslash\backslash\backslash\backslash} \qquad (32)$$

$$\alpha_2 u_{f0}^{\backslash\backslash} - R_e u_{f0}^{\backslash} - (\alpha_1 + i\omega R_e) u_{f0} = B \qquad (33)$$

$$\alpha_2 u_{f1}^{\backslash\backslash} - R_e u_{f1}^{\backslash} - (\alpha_1 + i\omega R_e) u_{f1} = -u_{f0}^{\backslash\backslash\backslash\backslash} \qquad (34)$$

While the boundary conditions will take the following form:

$$\left.\begin{array}{lllll} u_{s0} = 0, & u_{s1} = 0, & T_s = 1, & C_s = 1, & at \quad y = 1 \\ u_{s0} = 0, & u_{s1} = 0, & T_s = 0, & C_s = 0, & at \quad y = 0 \\ u_{f0} = 1, & u_{f1} = 0, & T_f = 1, & C_f = 1, & at \quad y = 1 \\ u_{f0} = 1, & u_{f1} = 0, & T_f = 0, & C_f = 0, & at \quad y = 0 \end{array}\right\} \qquad (35)$$

Hence, the solutions of equations ((23)-(28)) subject to boundary conditions (35) can be obtained as follows respectively:

4.3 Steady case

$$u_{s0} = \mathrm{c}_1 e^{m_1 y} + \mathrm{c}_2 e^{m_2 y} - \frac{A}{\alpha_1} \qquad (36)$$

$$u_{s1} = (\mathrm{c}_3 + \beta_1) e^{m_1 y} + (\mathrm{c}_4 + \beta_2) e^{m_2 y} \qquad (37)$$

$$T_s = \mathrm{c}_9 e^{m_9 y} + \mathrm{c}_{10} e^{m_{10} y} \qquad (38)$$

$$C_s = c_{13}e^{m_{13}y} + c_{14}e^{m_{14}y} + \beta_5 e^{m_9 y} + \beta_6 e^{m_{10}y} \quad (39)$$

4.4 Unsteady case

$$u_{f0} = c_5\, e^{m_7 y} + c_6 e^{m_8 y} \quad (40)$$

$$u_{f1} = (c_7 + \beta_3)e^{m_7 y} + (c_8 + \beta_4)e^{m_8 y} \quad (41)$$

$$T_f = c_{11}e^{m_{11}y} + c_{12}e^{m_{12}y} \quad (42)$$

$$C_f = c_{15}e^{m_{15}y} + c_{16}e^{m_{16}y} + \beta_7 e^{m_9 y} + \beta_8 e^{m_{10}y} \quad (43)$$

5. Results and discussion

The problem of an incompressible unsteady (MHD) pulsatile flow of couple-stress non-Newtonian fluid obeying Casson model through a porous medium with heat and mass transfer in two-dimensional channel using homotopy perturbation expansion has been studied. We discussed the influences of the magnetic field and porosity of the medium on the fluid. The formula of the velocity, temperature and concentration have been obtained. Different parameters of the problem have been showed graphically such as the magnetic parameter M^2, permeability of the porous media parameter k_p ,the couple stress parameter R_c ,the parameter of non-Newtonian fluid β , Prandtl number P_r, and S_c Shmidt number and the chemical reaction ξ.

Figure (4.2) illustrates the change of the velocity distribution u versus the coordinate y with several value of R_e. It is clear in figure (4.2) that the velocity increases in the region $0 < y < 0.5$, when the Reynolds number R_e increases. But the velocity decrease in the region $0.5 < y < 1$ as the Reynolds number R_e increases. We can observe from figure (4.3) that the velocity u increases with the increases of R_e according to the time variation. The effect permeability of the porous media parameter k_p on the velocity distribution is indicated in figures (4.4) and (4.5) . It is found that the velocity distribution increases with increasing k_p versus the coordinate y in figure (4.4) but k_p behave the opposite behavior according to the time variation in figure (4.5). Figures ((4.6) and (4.8)) illustrate the effects of the parameter of non-Newtonian fluid β and magnetic parameter M respectively on the velocity distribution. it is clear that the velocity distribution decreases with the increases of β and M on the coordinate y , in figure (4.7) the velocity distribution increases (decreases) with the increases of β but the velocity distribution increases with the increases of M in figure (4.9) according to the time variation. Figures (4.10) and (4.11) show the relation between the velocity distribution and the couple stress parameter R_c . It is observed that the velocity distribution decreases with the increasing R_c according to the coordinate y and the time variation.

The relation between temperature distributions T versus Reynolds number R_e and Prandtl number P_r respectively has been presented in figures ((4.12) - (4.15)) where the temperature distributions T decreases with the increasing of number R_e and P_r according to coordinate y in figures ((4.12) and (4.14)) , and temperature distributions T decreases with the increasing of number R_e and P_r according to the time t. The relation between temperature distributions T and heat radiation coefficient N has been presented in figures ((4.16) and (4.17)) where the temperature distributions T increases with the increasing of heat radiation coefficient N according to coordinate y in figures (4.16) and increases with the increasing of heat radiation coefficient N according to time variation in figures (4.17). The last parameter we investigate it with temperature distributions T is heat absorption coefficient γ , in figures ((4.18) and (4.19)) we found that the temperature distributions T increases with the increases of γ according to both of the coordinate y and the time variation.

We have different graphs in figures ((4.20)-(4.27)). It is illustrate the behavior of concentration distributions C versus the coordinate y and time t with the changing in parameters Reynolds number R_e, Schmidt number S_c, chemical reaction ξ and Soret number S_r. The relation between concentration distributions C versus Reynolds number R_e and chemical reaction ξ respectively has been presented in figures ((4.20) and (4.24)) where the concentration distributions C decreases with the increasing of Reynolds number R_e and chemical reaction ξ . in figure (4.22) concentration distributions C decreases in the region $0 < y < 0.7$, when the Schmidt number S_c increases. But the concentration distributions C increase in the region $0.7 < y < 1$ as the Schmidt number S_c increases, according the coordinate y. also in figure (4.26) concentration distributions C increases with the increasing of Soret number S_r. In figures ((4.21) and (4.23)) shows the Concentration distributions C for different values of Reynolds number R_e and Schmidt number S_c according to the time variation. Where the concentration distributions C increases with the increases of R_e and S_c . While in figure (4.25), it is found that the concentration distributions C increases (decreases) with the increases of ξ according to the time. It is observed that the concentration distributions C decreases as the Soret number S_r increases according to time in figure (4.27).

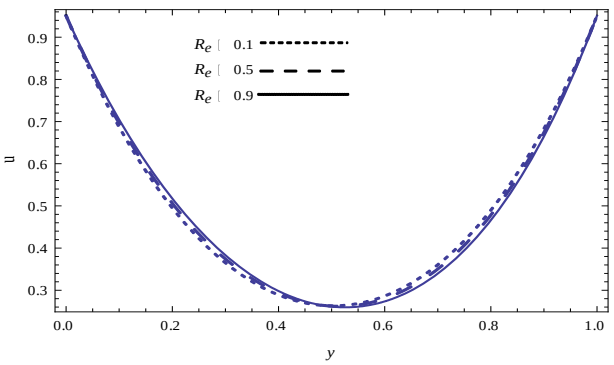

Figure 2: The velocity distribution u is plotted with the coordinates y for different values of Reynolds number R_e

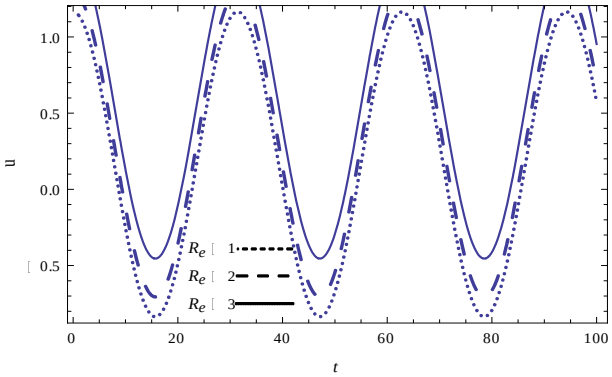

Figure 3: The velocity distribution u is plotted with the time t for different values of Reynolds number R_e

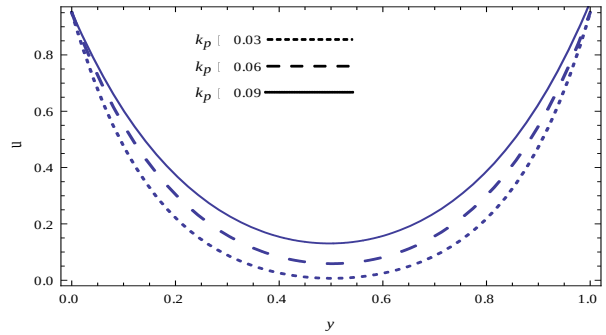

Figure 4: The velocity distribution u is plotted with the coordinates y for different values of permeability parameter k_p

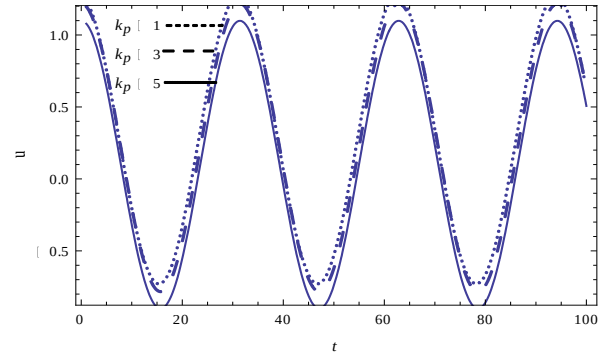

Figure 5: The velocity distribution u is plotted with the time t for different values of permeability parameter k_p

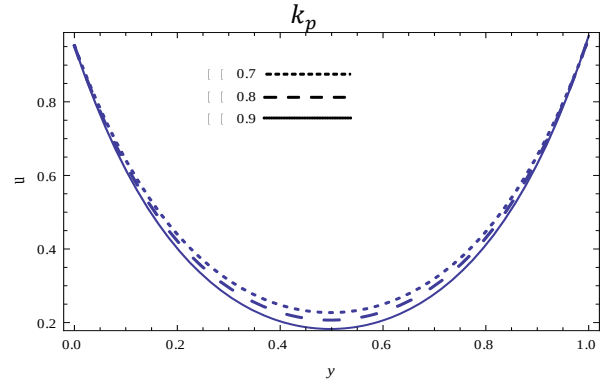

Figure 6: The velocity distribution u is plotted with the coordinates y for different values of material parameter β

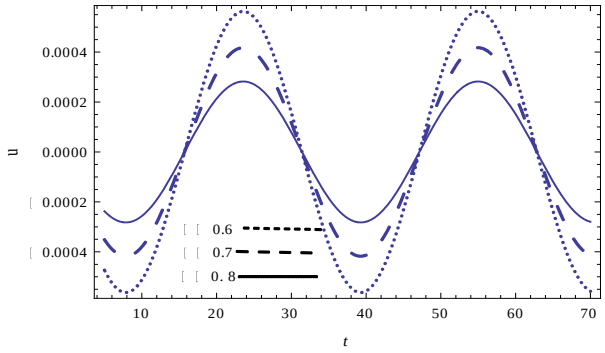

Figure 7: The velocity distribution u is plotted with the time t for different values of material parameter β

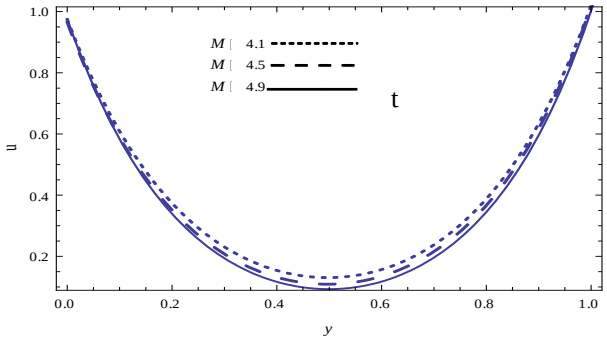

Figure 8: The velocity distribution u is plotted with the coordinates y for different values of magnetic field parameter M

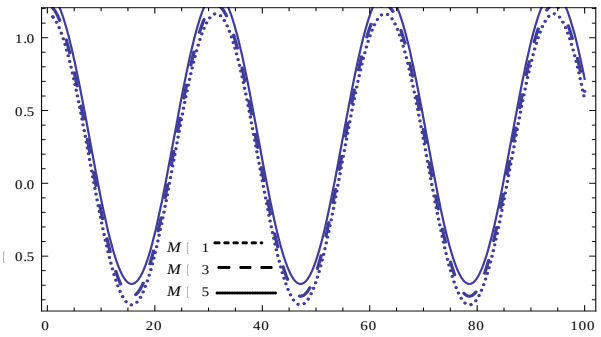

Figure 9: The velocity distribution u is plotted with the time t for different values of magnetic field parameter M

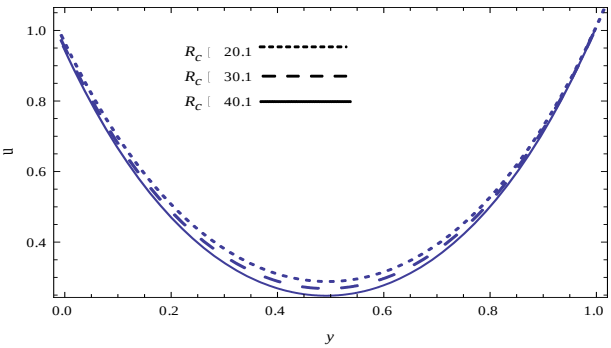

Figure 10: The velocity distribution u is plotted with the coordinates y for different values of couple stress parameter R_c

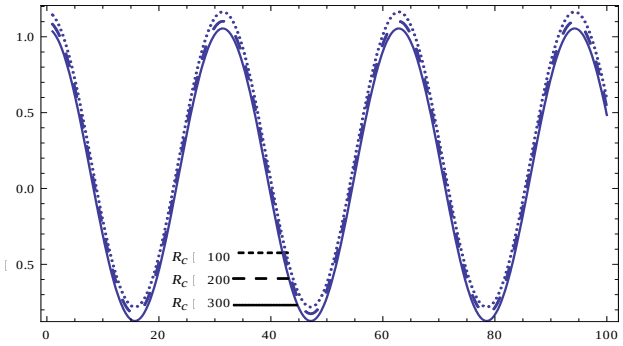

Figure 11: The velocity distribution u is plotted with the coordinates y for different values of couple stress parameter R_c

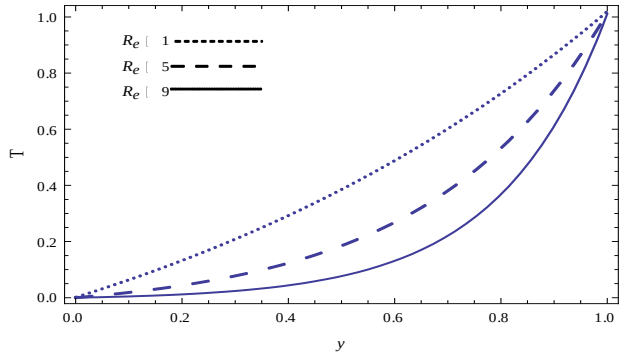

Figure 12: The temperature distribution T is plotted with the coordinates y for different values of Reynolds number R_e

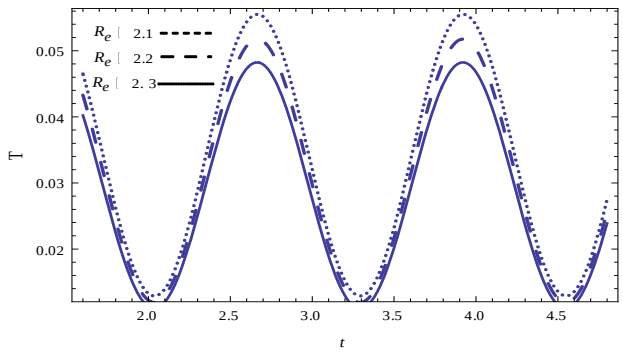

Figure 13: The temperature distribution T is plotted with the coordinates y for different values of Reynolds number R_e

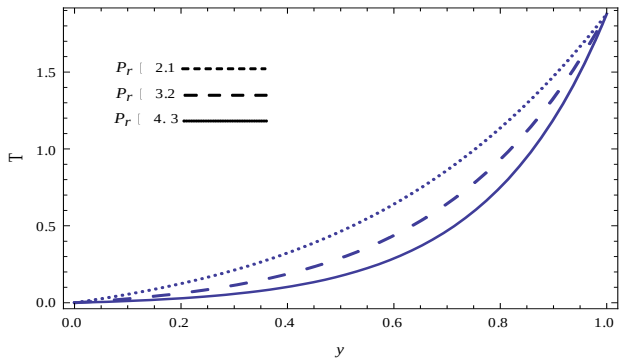

Figure 14: The temperature distribution T is plotted with the coordinates y for different values of Prandtl number P_r

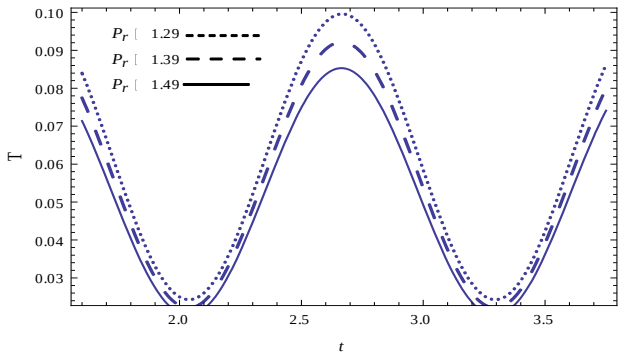

Figure 15: The temperature distribution T is plotted with the coordinates y for different values of Prandtl number P_r

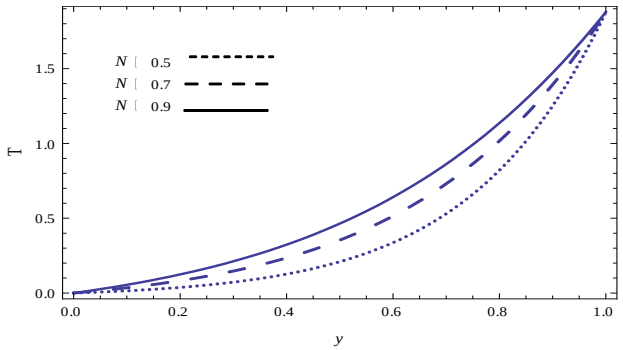

Figure 16: The temperature distribution T is plotted with the coordinates y for different values of radiation coefficient N

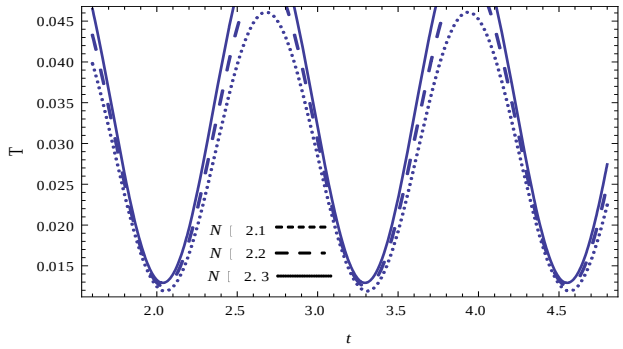

Figure 17: The temperature distribution T is plotted with the coordinates y for different values of radiation coefficient N

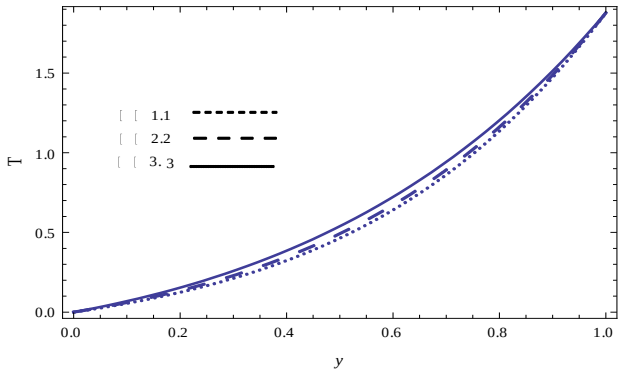

Figure 18: The temperature distribution T is plotted with the coordinates y for different values of is heat absorption coefficient γ

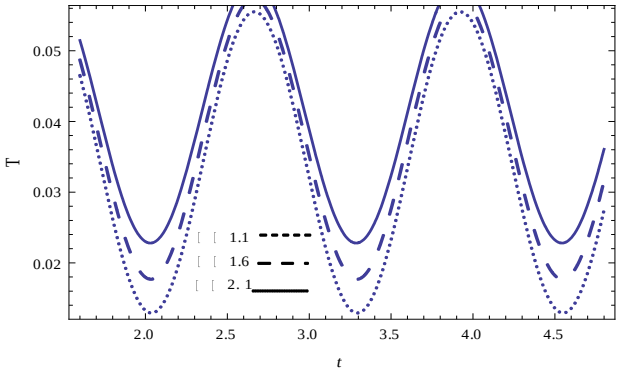

Figure 19: The temperature distribution T is plotted with the coordinates y for different values of heat absorption coefficient γ

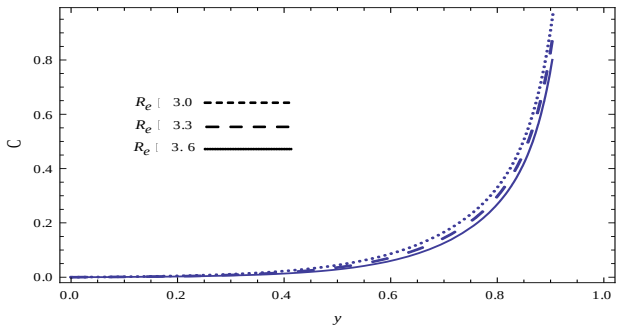

Figure 20: The concentration distributions C is plotted with the coordinates y for different values of Reynolds number R_e

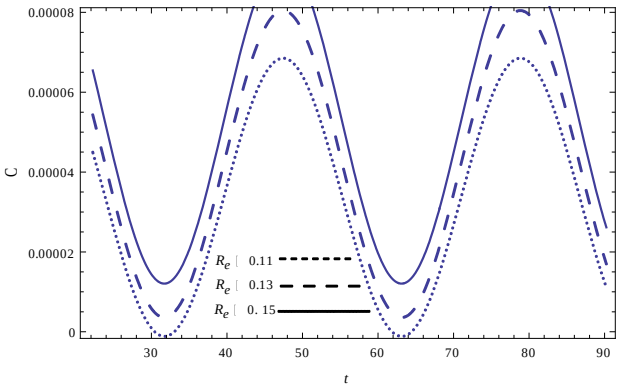

Figure 21: The concentration distributions C is plotted with the coordinates y for different values of Reynolds number R_e

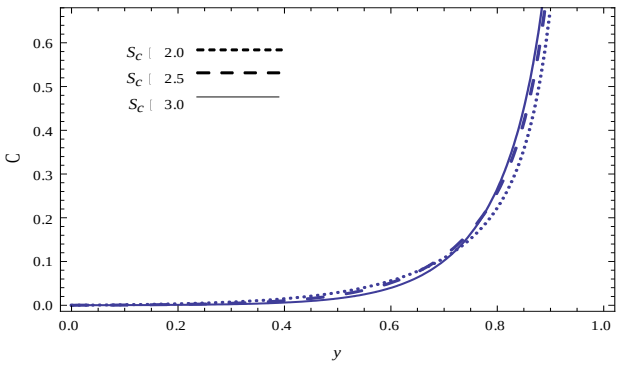

Figure 22: The concentration distribution C is plotted with the coordinates y for different values of Schmidt number S_c

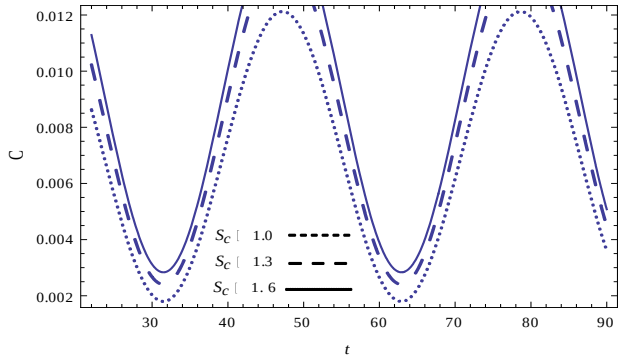

Figure 23: The concentration distribution C is plotted with the time t for different values of Schmidt number S_c

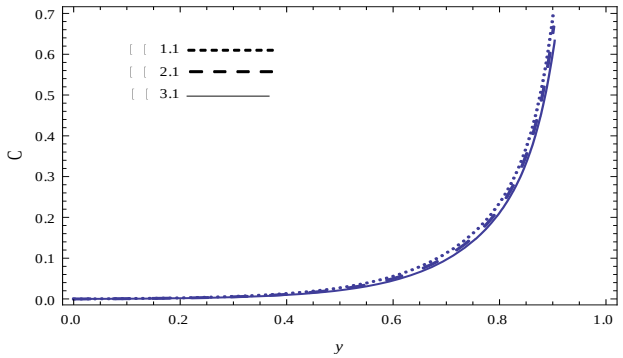

Figure 24: The concentration distribution C is plotted with the coordinates y for different values of chemical reaction ξ

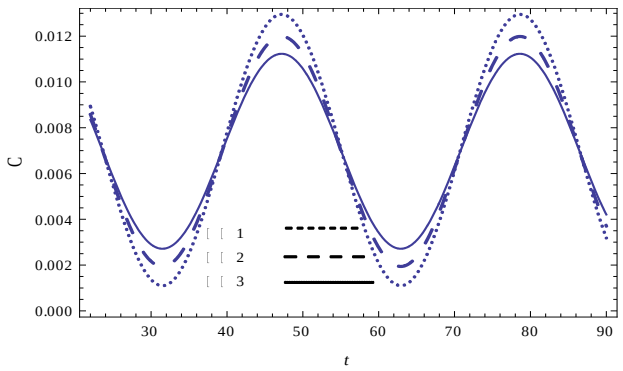

Figure 25: The concentration distribution C is plotted with the time t for different values of chemical reaction ξ

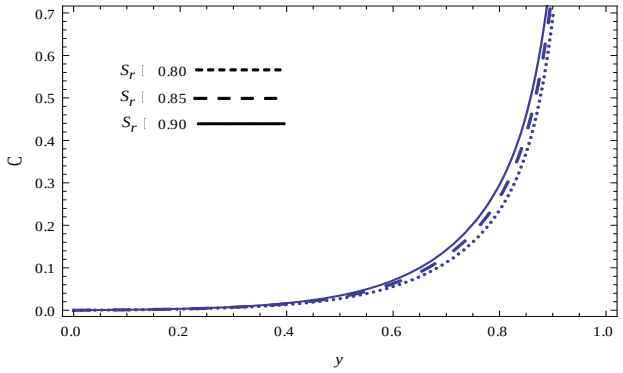

Figure 26: The concentration distribution C is plotted with the coordinates y for different values of Soret number S_r

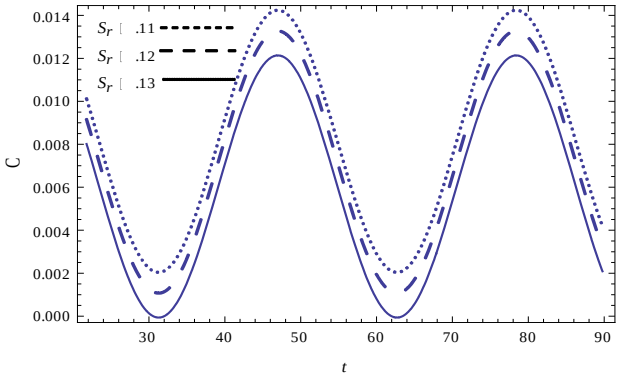

Figure 27: The concentration distribution C is plotted with the time t for different values of Soret number S_r

Conclusion

Because of the great importance in studying the Casson fluid through pours medium , specially in scientific and medical applications because the blood is kind of these fluids , the present study is modulated to treat this phenomenon. The problem considered the influence of the magnetic field. Through the present investigation, we have studied a Casson fluid, in the presence of mass and heat transfer in porous medium. The problem is modulated as a channel of width h . The mathematical analysis considered the governing equations of motion in analogy. Through the present investigation, we have studied the fluid with the appropriate boundary conditions. The model deals with the MHD dispersion in case of the unsteady state.

Because of the shortened of the difficulty of solving the differential equation of the problem, we are forced to use a homotopy perturbation technique which based on finding small parameter. This technique enable us to obtain the complete solution. The analytical results, yield the distributions of velocity, temperature and concentration. To clarify the influences of the various parameters of the problem at hand, a numerical calculating is made. The concluding remarks may be listed as follows.

1) The velocity distribution u of the fluid has the same behavior with y-coordinate and time t. It decreases with the increase of k_p.
2) The velocity distribution u of the fluid has different behavior with M^2 and material parameter β . It increases with the increase of M^2 and β.
3) The results which obtained in the steady state for boundary conditions agreed with both of M. Gowdara *et al.* and V. Ramachandra. where the velocity distribution u of the fluid in the steady state has the same behavior with magnetic field parameter M^2 and k_p.

Reference

Kh.S. Mekheimer (2008) Effect of the induced magnetic field on peristaltic flow of a couple stress fluid. Physics Letters A. Vol. 372, pp. 4271–4278.

Asma Khalid, Ilyas Khan, Arshad Khan, Sharidan Shafie (2015) Unsteady MHD free convection flow of Casson fluid past over an oscillating vertical plate embedded in a porous medium. Engineering Science and Technology, an International Journal Vol. 371, pp. 1-9

G. Mahanta, S. Shaw (2015) 3D Casson fluid flow past a porous linearly stretching sheet with convective boundary condition Alexandria Engineering Journal, in press.

Swati Mukhopadhyay, Prativa Ranjan, Krishnendu Bhattacharyy, G.C. Layek (2013)Casson fluid flow over an unsteady stretching surface Ain Shams Engineering Journal, Vol. 4, pp. 933–938.

Naveed Ahmed a , Umar Khan , Sheikh Irfanullah Khan, Saima Bano, Syed Tauseef Mohyud-Din (2015) Effects on magnetic field in squeezing flow of a Casson fluid between parallel plates Journal of King Saud University , in press.

S.K. Gupta, T.R.D. Patel, R.C. Ackerberg (2013) Wall heat/mass transfer in pulsatile flow Chemical Engineering Science, Vol. 37, pp. 1727–1739.

Pingping Ma, Xianming Li, David N. Ku (1994) Heat and mass transfer in a separated flow region for high Prandtl and Schmidt numbers under pulsatile conditions. Vol. 37, Pages 2723–2736.

G.C. Shit , Sreeparna Majee (2015) Pulsatile flow of blood and heat transfer with variable viscosity under magnetic and vibration environment Journal of Magnetism and Magnetic Materials. Vol. 388, Pages 106–115,

S. Srinivas a , T. Malathy b , A. Subramanyam Reddy (2015) A note on thermal-diffusion and chemical reaction effects on MHD pulsating flow in a porous channel with slip and convective boundary conditions Journal of King Saud University Engineering Sciences in press.

M. Gowdara, Pavithra, Bijjanal J. Gireesha (2014)., Unsteady flow and heat transfer of a fluid-particle over an exponentially stretching sheet Ain Shams Engineering Journal Vol. 5, Pages 613–624

V. Ramachandra , N. Bhaskar Reddy (2007) Radiation and mass transfer on an unsteady MHD free convection °ow past a heated vertical plate in a porous medium with viscous dissipation applied mechanic., Vol. 34, Pages 135–160.